Chapter 31

ING Rhythms

Gamma rhythms can also be generated by the interaction of I-cells alone, without any involvement of E-cells. For example, in brain slices, gamma rhythms can be evoked even in the presence of drugs blocking AMPA and NMDA receptors. See Fig. 31.1 for an example, recorded from rat CA1.

Assuming strong external drive to the I-cells, the mechanism seems, at first sight, similar to PING: Activity of the I-cells creates inhibition, which silences the entire population temporarily, and when firing resumes, it is in greater synchrony, as described in Chapter 29.[25] Gamma rhythms created in this way were called *Interneuronal Network Gamma (ING)* rhythms in [183]; earlier studies of such rhythms include [174] and [182].

To construct model networks of inhibitory cells, we simply omit the E-cells from the networks of Chapter 30 and strengthen the external drive to the I-cells. The resulting networks are capable of generating gamma rhythms, but only under idealized circumstances, namely with little heterogeneity in external drives (σ_I small) and very little randomness in synaptic connectivity (p_{II} very close to 1); see Sections 31.1 and 31.2 for examples.

The fast-firing interneurons involved in generating gamma rhythms are well known to be connected by gap junctions [57]. When gap-junctional coupling is added to the model networks, ING rhythms become much more robust; this is demonstrated with examples in Section 31.3. It is in line with many experimental and modeling studies that have found gap junctions to drive neurons towards

---

[25]This requires that inhibitory input in fact delays and synchronizes I-cell firing. For example, an h-current in the I-cells may undermine the mechanism, just as an h-current in the E-cells can undermine PING. However, in this chapter, we will take the I-cells to be WB neurons, for which there are no such complications.

269
C. Börgers, *An Introduction to Modeling Neuronal Dynamics*,
Texts in Applied Mathematics 66, DOI 10.1007/978-3-319-51171-9_31

synchrony (see, for instance, [93, 153, 160]), and is expected because of the equili-brating effect of discrete diffusion (see Chapter 21).[26]

Even in the absence of any heterogeneity, ING networks without gap junctions can generate *clustering*, with individual cells firing only on a fraction (most typically
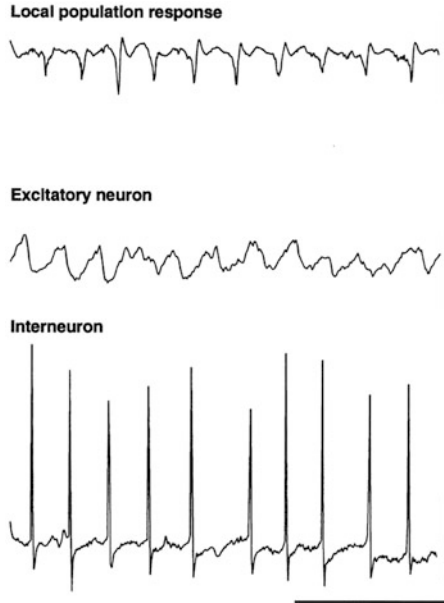
Figure 31.1. *Figure 3 of [183], reproduced with publisher's permission. These are* in vitro *recordings from rat CA1. AMPA and NMDA receptors were blocked by drugs, and the inhibitory interneurons were excited using a technique called pressure ejection of glutamate. The figure shows a local field potential (top trace), and membrane potentials of a pyramidal cell and an inhibitory interneuron (middle and bottom traces). The three traces were not recorded concurrently. The horizontal scale bar indicates 100 ms. The vertical scale bars indicate 1 mV (top trace), 4 mV (middle trace), and 20 mV (bottom trace).*

one half) of the population spike volleys. This was shown in [174] (and also, for purely inhibition-based rhythms at lower frequencies, earlier in [62]). We show examples in Section 31.4.

In summary, synchrony in networks of inhibitory cells without gap-junctional coupling seems fairly fragile. In Section 31.5, we illustrate this point in yet another way, using the example of a pair of abstract oscillators coupled by inhibitory pulses.

---

[26]It is not, however, *obvious* that the equilibrating effect of discrete diffusion carries over to the case of spiking neurons, and in fact it is not always true; see [28, Fig. 8].

31.1 Single-Cell ING

To build intuition, we begin with a single WB neuron with an inhibitory autapse. A voltage trace resulting from a simulation of such a single-cell "network" model is shown in Fig. 31.2; the parameter values are specified in the caption of the figure. Not surprisingly, the voltage trace does not look much different from that of a WB neuron without the autapse.
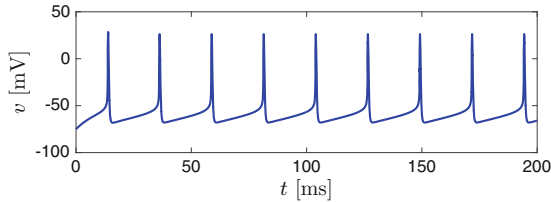
Figure 31.2. *Voltage trace of a WB neuron with an inhibitory autapse. The external drive is $I = 1.5$. The parameters characterizing the autapse are $\overline{g}_{syn} = 0.5$, $\tau_r = \tau_{peak} = 0.5$, $\tau_d = 9$, and $v_{rev} = -75$.* [1_CELL_ING]

We denote the period at which the cell in Fig. 31.2 fires by P, and explore the parameter dependence of P. In analogy with Table 30.1, we compute the percentage change in P resulting from a 1% reduction in I, a 1% increase in $\overline{g}_{syn}$, and a 1% increase in τ_d. Again we find that the period depends more sensitively on external drive than on the strength or decay time constant of the autapse.

|	$I \to 0.99I$	$\overline{g}_{syn} \to 1.01\overline{g}_{syn}$	$\tau_d \to 1.01\tau_d$
increase in P:	0.77	0.35	0.47

Table 31.1. *Parameter dependence of the period P of the rhythm of Fig. 31.2.* [1_CELL_ING_CONDITION_NUMBERS]

31.2 Basic Network Simulations

Figure 31.3 shows an ING rhythm generated by 100 WB neurons coupled with inhibitory synapses. Note that it takes longer to reach synchrony than in, for instance, the PING network of Fig. 30.4. In Fig. 31.3, conditions for synchronization are ideal: There is no heterogeneity in external drives, synaptic connectivity is all-to-all, and all synapses have the same strength. This is why *perfect* synchrony is reached in the limit as $t \to \infty$. With a modest level of drive heterogeneity ($\sigma_I = 0.03$), it takes even longer to reach (approximate) synchrony; see Fig. 31.4. A similar effect is seen when 15% of the synaptic connections in Fig. 31.3 are omitted at random ($p_{II} = 0.85$), and the remaining ones strengthened by the factor 100/85; see Fig. 31.5. As in Chapter 30, this is not primarily an effect of sparseness and randomness *per se*, but of variations in the total amount of synaptic input per cell; see Fig. 31.6. With greater heterogeneity, the rhythm disappears; see Fig. 31.7, and also exercise 3. For an analysis of the sensitivity of ING rhythms to heterogeneity, see [178].
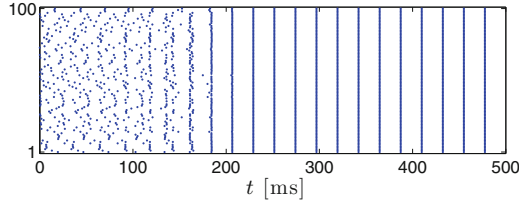
Figure 31.3. *Spike rastergram of 100 synaptically coupled WB neurons. Spike times of I-cells (which are the only cells in the network) are indicated in blue. The parameters, using the notation of Chapter 30, are $N_I = 100$, $\overline{I}_I = 1.5$, $\hat{g}_{II} = 0.5$, $p_{II} = 1$, $\tau_{r,I} = 0.5$, $\tau_{\mathrm{peak},I} = 0.5$, $\tau_{d,I} = 9$, $v_{\mathrm{rev},I} = -75$. There is no heterogeneity of any kind in the network. Initialization is, as in Chapter 30, asynchronous, in the sense explained in Section 24.1.* [ING_1]
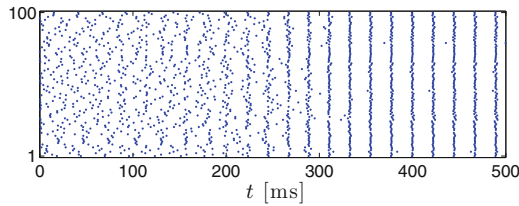

Figure 31.4. *Same as Fig. 31.3, but with heterogeneous external drive (different neurons receive different, temporally constant drives): $\sigma_I = 0.03$.* [ING_2]
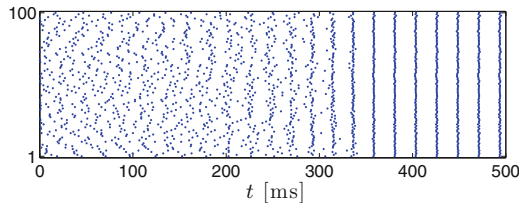

Figure 31.5. *Same as Fig. 31.3, but with 15% of synaptic connections omitted at random ($p_{II} = 0.85$), and the remaining ones strengthened by the factor 100/85.* [ING_3]

Several studies have suggested, based on both experiments and simulations, that parameter choices such as those in Figs. 31.3–31.7 might be far from realistic, and that the inhibitory synapses should be briefer, stronger, and shunting rather than hyperpolarizing; see in particular [7] and [169]. We will not discuss this point further here, and leave it to the reader to investigate ING rhythms with briefer, stronger, shunting inhibition; see exercise 12.
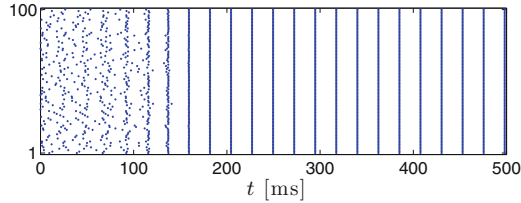
Figure 31.6. *Same as Fig. 31.5, but now each cell receives inputs from exactly 85 cells, instead of receiving input from a random number of cells with mean 85.* [`ING_4`]
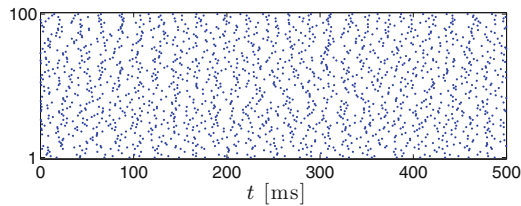
Figure 31.7. *As in Fig. 31.3, but with $\sigma_I = 0.05$ and $p_{II} = 0.5$* [`ING_5`]

31.3 Adding Gap Junctions

We model gap junctions as described in Chapter 21. In our code, the strength of the connection between neurons i and j is taken to be

$$g_{\mathrm{gap},ij} = \left\{ \begin{array}{ll} \hat{g}_{\mathrm{gap}} / \left(p_{\mathrm{gap}}(N_I - 1) \right) & \text{with probability } p_{\mathrm{gap}}, \\ 0 & \text{with probability } 1 - p_{\mathrm{gap}}, \end{array} \right.$$

for $i > j$, $g_{\mathrm{gap},ij} = g_{\mathrm{gap},ji}$ for $i < j$, and $g_{\mathrm{gap},ii} = 0$. The parameter p_{gap} determines the density of gap-junctional connections, and $\hat{g}_{\mathrm{gap}}$ determines their strength. We scale by $p_{\mathrm{gap}}(N_I - 1)$ to make the expected value of the total gap-junctional conductance affecting a cell independent of p_{gap} and N_I; compare the discussion in Section 30.2. (Note that a cell can receive gap-junctional input only from *other* cells, not from itself. This is why we scale by $p_{\mathrm{gap}}(N_I - 1)$ here, not by $p_{\mathrm{gap}}N_I$.) In the simulations presented here, we use $N_I = 100$ and $p_{\mathrm{gap}} = 0.05$, so the expected number of gap-junctional contacts per cell is $99 \times 0.05 = 4.95 \approx 5$, and $\hat{g}_{\mathrm{gap}} = 0.1$, so the strength of each gap-junctional connection is $g_{\mathrm{gap},ij} \approx 0.02$. With this gap-junctional coupling added, (approximate) synchrony is reached extremely rapidly, within two gamma cycles, in the simulations of Figs. 31.4 and 31.5 (exercise 2), and even a much greater degree of heterogeneity does not destroy the rhythm; see Fig. 31.8.

31.4 Clustering

Even in purely inhibitory networks without any heterogeneity, synchronization is somewhat fragile in the absence of gap junctions. There are parameter choices for
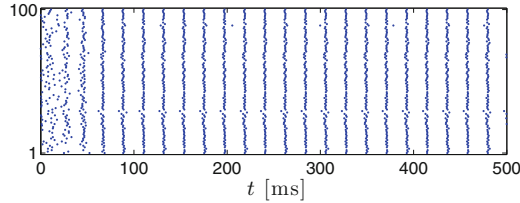
Figure 31.8. *As in Fig. 31.7, but with $\hat{g}_{\mathrm{gap}} = 0.1$ and $p_{\mathrm{gap}} = 0.05$.* [`ING_6`]

which one sees a breakup of the cells into $n > 1$ clusters (usually $n = 2$, but see exercise 7), with each cluster firing on every n-th population cycle. However, the clustering behavior is fragile as well: A moderate amount of drive heterogeneity destroys it, and gap-junctional coupling does *not* restore it, but instead results in complete synchronization, even for parameters for which there is clustering in the absence of heterogeneity. For these reasons, it seems unclear whether clustering in ING networks could have biological relevance. Nonetheless we will briefly discuss it here, as another illustration of the fragility of ING rhythms in the absence of gap junctions.

Wang and Buzsáki [174] demonstrated numerically that in networks without heterogeneity, clustering is seen when the hyperpolarization following firing is pronounced [174, Fig. 3], especially when the synaptic reversal potential is relatively high. The hyperpolarization following firing can be made pronounced by slowing down the variables h and n, which play central roles in ending the action potential; see [174], and also Exercise 5.6. If we multiply the functions α_h, β_h, α_n, and β_n by $1/2$ (this amounts to doubling τ_h and τ_n, or to reducing the scaling factor ϕ of [174] from 5 to 2.5), Fig. 31.3 turns into 31.9. The red rectangle in Fig. 31.9 is shown once more, enlarged, in Fig. 31.10. There are two clusters firing alternatingly.[27]
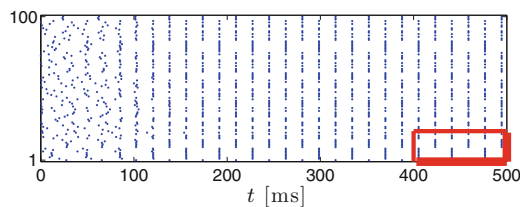

Figure 31.9. *As in Fig. 31.3, but with α_h, β_h, α_n, and β_n reduced by a factor of 2. The red rectangle indicates the window that is enlarged in Fig. 31.9.* [`ING_7`]

Heuristically, one can see why strong spike afterhyperpolarization and a relatively high synaptic reversal potential might counteract synchronization: Inhibition soon after firing is then *depolarizing*, since the membrane potential after firing will
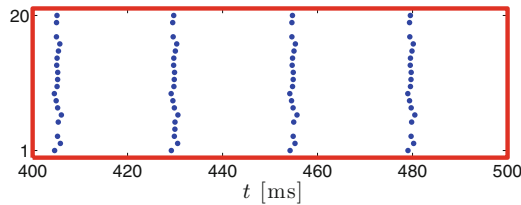
---

[27]If you conclude, after looking at Fig. 31.10, that something must be wrong with my code, download and examine the code, or do exercise 5, or both.
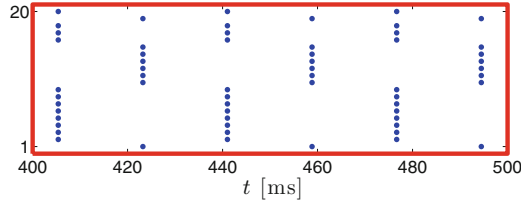
Figure 31.10. *Red window in Fig. 31.9, enlarged.* [ING_8]
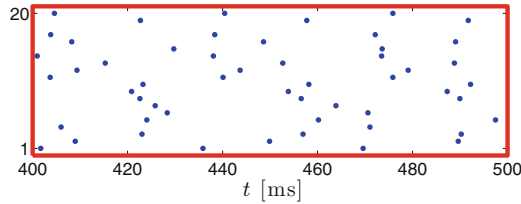
Figure 31.11. *Like Fig. 31.10, but with $\sigma_I = 0.05$.* [ING_9]

Figure 31.12. *Like Fig. 31.11, but with weak, sparse gap junctions: $\hat{g}_{\mathrm{gap}} = 0.04$, $p_{\mathrm{gap}} = 0.05$.* [ING_10]

be below the synaptic reversal potential, whereas inhibition arriving soon before firing will of course be *hyperpolarizing.* Consequently, the cells that fire first in an approximately (but not perfectly) synchronous spike volley accelerate each other by their inhibitory interactions, while slowing down the cells that are behind and receive the inhibition before firing.

When we introduce heterogeneity in drive ($\sigma_I = 0.05$) in the simulation of Fig. 31.9, the firing becomes asynchronous; see Fig. 31.11. When we add gap junctions, even quite weak and sparse ones, clustering does not return, but instead the entire population synchronizes; see Fig. 31.12.

You might wonder whether in a PING rhythm, clustering of the E-cells couldn't happen for the precisely same reason for which it happens in ING. In fact it can; see Chapter 32. For PING rhythms, clustering occurs easily when the E-cells express[28] adaptation currents. It is possible even without adaptation currents, but requires very rapid, and probably unrealistically rapid, inhibitory feedback; see Section 32.3.

---

[28]The word "express," used in this way, is useful neuroscience jargon. A cell in which a certain current is present is briefly said to "express" that current.

## 31.5   Two Abstract Oscillators Coupled by Inhibitory Pulses

Figure 25.10 shows a PRC of a WB neuron responding to a brief inhibitory pulse. We now consider a pair of abstract oscillators of the sort analyzed in Chapter 26, with a phase response function qualitatively resembling the function shown in Fig. 25.10. We define the phase response function by

$$g(\varphi) = -\mathcal{H}\left(\frac{\varphi - 0.1}{0.1}\right)\ \left(\mathcal{H}\left(\frac{0.8 - \varphi}{0.05}\right) - \mathcal{H}(-4)\right)\frac{\varphi}{2} \qquad (31.1)$$

with

$$\mathcal{H}(s) = \frac{1 + \tanh(s)}{2}. \qquad (31.2)$$

See exercise 8 for the motivation for this definition. Figure 31.13 shows the graph of g, and the graph of the function G derived from it as described in Section 26. Note that there is qualitative similarity between the graph of g and Fig. 25.10, but there is also a significant difference: In Fig. 25.10, $g(0) < 0$ (even an inhibitory pulse that arrives right at the moment at which the membrane potential crosses $-20\,\mathrm{mV}$ from above will retard the next spike), whereas in the framework of Chapter 26, $g(0) = g(1) = 0$. The graph of G shows that synchrony is weakly attracting (in fact, $G'(0) \approx 0.9467$, see exercise 9), but anti-synchrony is attracting as well. This is reminiscent of the network of Figs. 31.9 and 31.10, where clustering is a stable state, but so is synchrony (see exercise 6b). For further discussion of this example, see exercise 10.
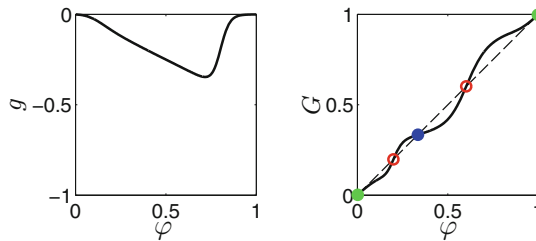

Figure 31.13. *The function g defined by eqs. (31.1) and (31.2), and the function G derived from it as described in Section 26. Fixed points of G correspond to possible phase-locked states of the two oscillators. Synchrony (solid green points) and anti-synchrony (solid blue point) are stable. There is another possible, but unstable phase-locked state (red circles).* [ABSTRACT_PULSE_COUPLING_INH]

Note that the value of φ corresponding to anti-synchrony in Fig. 31.13 is clearly not 1/2, contrary to what you might have expected. This is explained in the paragraph following the proof of Proposition 26.1.

31.6 Entrainment of Excitatory Cells by ING Rhythms

What happens when an ING network gives input to a population of other neurons, say a population of pyramidal cells? Is the rhythmicity projected into the target population? We can experiment by adding, for instance, to the network of Fig. 31.8, a population of E-cells, with $\hat{g}_{IE} > 0$ but $\hat{g}_{EI} = 0$, so that the E-cells are affected by, but do not affect the I-cells. If the E-cells receive too little external drive, then of course they will simply be suppressed by the inhibitory input. But given external drive sufficient to make them fire, will they fire rhythmically, phase-locked with the I-cells?
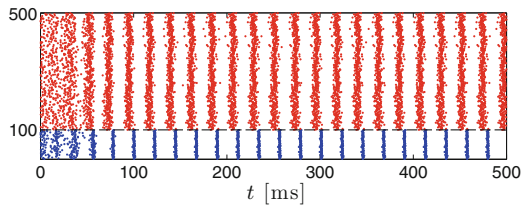
Figure 31.14. *The ING network of Fig. 31.8 entraining a population of $N_E = 400$ E-cells. Here $\hat{g}_{EE} = \hat{g}_{EI} = 0$, but $\hat{g}_{IE} = 0.5$, $p_{EI} = 0.5$, $\overline{I}_E = 1.5$, and $\sigma_E = 0.1$.* [ING_ENTRAINING_E_CELLS]
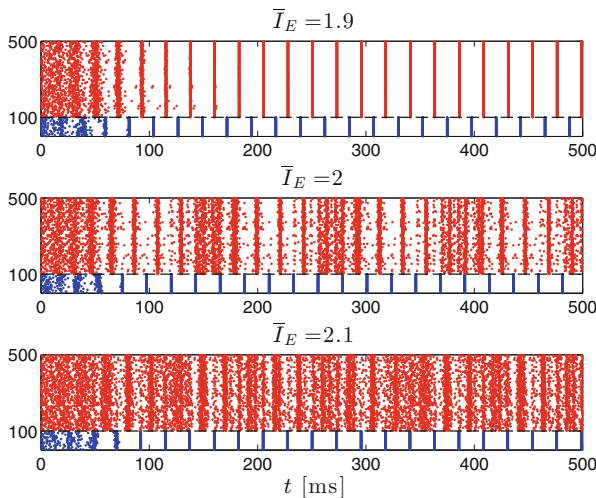
Figure 31.15. *Same network as in Fig. 31.14, with all heterogeneity in drives and randomness in connectivity removed ($\sigma_E = \sigma_I = 0$, $p_{II} = p_{IE} = 1$). As $\overline{I}_E$ crosses a threshold, phase-locking of the E-cell population with the I-cell population is lost.* [ING_ENTRAINING_E_CELLS_2]

Figure 31.14 shows a case in which the answer to the above question is "yes." Note that the firing looks very similar to that in a PING network, in spite of the fact that there is no E-to-I coupling. There is a broad range of drives to the E-cells for which similar patterns are obtained. As the drive to the E-cells gets stronger, the phase relation between E- and I-cells changes, with the E-cells firing earlier in the cycle of the I-cells; see upper panel of Fig. 31.15.

Then, as a threshold value is crossed, there is an abrupt transition from phase-locking of the E-cells with the I-cell to a "phase walkthrough" pattern, shown in the middle panel of Fig. 31.15. The E-cells fire earlier and earlier in the I-cell cycle, until they fire twice in one cycle, then return to firing later in the cycle, and the gradual shift to earlier phases resumes. For yet stronger drive, there is greater irregularity; see bottom panel of Fig. 31.15. To separate the effect of a strong drive to the E-cells from the effects of heterogeneity in drives and randomness in connectivity, drive heterogeneity and randomness of connectivity were omitted in Fig. 31.15.

Exercises

31.1. (∗) Compute tables similar to Table 31.1 for other parameter values. Also investigate how sensitively P depends on other parameters, for instance, on $\overline{g}_L$.

31.2. (∗) Add gap junctions with $\hat{g}_{\text{gap}} = 0.1$ and $p_{\text{gap}} = 0.05$ to the codes generating Figs. 31.4 and 31.5, and see what you get. (Hint: This is already programmed in the codes generating Figs. 31.4 and 31.5, all you need to do is make $\hat{g}_{\text{gap}}$ non-zero!)

31.3. (∗) In the code that generates Fig. 31.7, change the initialization so that each neuron is initialized at a random phase uniformly distributed not in $[0, 1]$, but in $[0, 0.02]$. Thus the population is nearly synchronous at the beginning. How does the rastergram change? Does (approximate) synchrony appear to be stable?

31.4. (∗) To which extent does the rhythm in Fig. 31.8 depend on the chemical synapses? Would the neurons similarly synchronize, because of the gap junctions, even if $\hat{g}_{II}$ were zero?

31.5. (∗) When you look at Figs. 31.9 and 31.10, do you think something must be wrong? I did, when I first saw these figures. There are strangely long sequences of neurons with consecutive indices that belong to the same cluster. It looks as though neurons with nearby indices were correlated. But membership in clusters should really be random here, shouldn't it? There should be no correlation between the cluster that neuron i belongs to, and the cluster that neuron $i + 1$ belongs to.

To reassure yourself that nothing is alarming about Fig. 31.9, define

$$f(i) = \left\{ \begin{array}{ll} 1 & \text{with probability } 1/2, \\ 2 & \text{with probability } 1/2, \end{array} \right. \quad i = 1, 2, \dots, 20,$$

and plot $f(i)$ as a function of i. Compute several realizations of f, of course using different random number generator seeds each time. (All you need to do in Matlab to get different realizations of f is not reset the seed before computing a new realization.) Do you see plateaus that seem surprisingly long, suggesting a correlation between $f(i)$ and $f(i+1)$?

The phenomenon that you see here is well-known in sports: Fairly long "winning streaks" and "losing streaks" are more likely to emerge by pure chance than most of us would expect [59].

31.6. (∗) (a) Does the clustering shown in Fig. 31.10 persist for a much longer time? Run the simulation for 2000 ms, and see whether you still observe the same clusters as in Fig. 31.10 in the last 100 ms of simulated time. (b) Repeat the simulation of Fig. 31.10 with initial conditions close to synchrony. (For instance, start all neurons at phases selected with uniform distribution from the interval [0, 0.1].) Do you get clustering, as in Fig. 31.10?

31.7. (∗) In the code that generates Fig. 31.10, use the parameters $\tau_{r,I} = 0.2$, $\tau_{\text{peak},I} = 0.2$, $\tau_{d,I} = 1$. (These values are admittedly implausible biologically.) Show that you get three clusters.

31.8. (a) Plot the function $\mathcal{H}$ defined in eq. (31.2). (b) Explain what motivates the definition (31.1).

31.9. (∗) Use the code that generates Fig. 31.13 to verify that $G'(0) \approx 0.9467$.
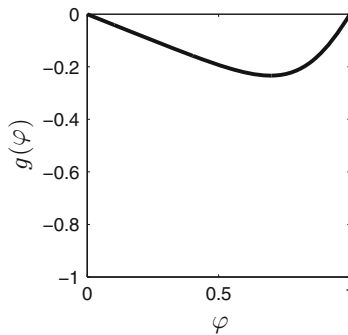
Figure 31.16. *A simplification of the function g in Fig. 31.13.*
[ABSTRACT_PULSE_COUPLING_INH_2]

31.10. (†) Figure 31.16 shows a phase response function qualitatively similar to that in Fig. 31.13, but with simpler behavior near $\varphi = 0$ and 1. The behavior of g near 0 and 1 determines the stability of synchrony; see (26.10). The stability of non-synchronous phase-locked states, on the other hand, is determined by the behavior away from the edges. So by analyzing non-synchronous phase-locked states for the PRC shown in 31.16, we can understand non-synchronous phase-locked states for the PRC in Fig. 31.13.

Assume that $g(\varphi) = \epsilon g_0(\varphi)$, where $\epsilon \in (0, 1]$, and $g_0 = g_0(\varphi)$, $\varphi \in [0, 1]$, is a continuously differentiable function with $g_0(0) = g_0(1) = 0$, $g_0(\varphi) < 0$ for $\varphi \in (0, 1)$, and $|g'(0)| < g'(1)$.

(a) Show that synchrony is unstable for sufficiently small $\epsilon \in (0, 1]$.

(b) Assume that the function G, derived from g as in Chapter 26, has finitely many fixed points only. Show that there is a stable non-synchronous phase-locked state.

31.11. ($*$) Test what happens when one makes $\overline{I}_E$ much smaller in the simulations of Fig. 31.15. Find various possible entrainment patterns by varying $\overline{I}_E$.

31.12. ($*$) Investigate ING rhythms with briefer, stronger, shunting inhibition, and compare their properties with those of the ING rhythms studied in this chapter, using variations on the codes generating the figures in this chapter.